HHS Public Access

Author manuscript

ACS Appl Mater Interfaces. Author manuscript; available in PMC 2022 June 27.

Published in final edited form as:

ACS Appl Mater Interfaces. 2022 May 04; 14(17): 19104–19115. doi:10.1021/acsami.1c24113.

Subcutaneous Administration of Nitric Oxide-Releasing Nanomatrix Gel Ameliorates Obesity and Insulin Resistance in High Fat Diet-induced Obese Mice

Guang Ren[1],

Patrick Tae Joon Hwang[2],

Reid Millican[2],

Juhee Shin[3],

Brigitta C. Brott[2,4],

Thomas van Groen[5],

Craig M. Powell[5],

Sushant Bhatnagar[1,6],

Martin E. Young[4,6],

Ho-Wook Jun[2,3],

Jeong-a Kim[1,6,*]

[1]Department of Medicine, Division of Endocrinology, Diabetes, and Metabolism, University of Alabama at Birmingham, Birmingham, AL 35294

[2]Endomimetics, LLC, Birmingham, AL 35242

[3]Department of Biomedical engineering, University of Alabama at Birmingham, Birmingham, AL 35294

[4]Division of Cardiovascular Disease, University of Alabama at Birmingham, Birmingham, AL 35294

[5]Department of Neurobiology, University of Alabama at Birmingham, Birmingham, AL 35294

[6]UAB Comprehensive Diabetes Center, University of Alabama at Birmingham, Birmingham, AL 35294

Abstract

Nitric oxide (NO) is a gaseous signaling molecule, which plays crucial roles in various biological processes, including inflammatory responses, metabolism, cardiovascular functions, and cognitive function. NO bioavailability is reduced with aging and cardiometabolic disorders in humans and

[*]**Address correspondence to:** Department of Medicine, Division of Endocrinology, Diabetes, and Metabolism, University of Alabama at Birmingham, Birmingham, Alabama 35294 USA Tel. 205-934-4128, Fax 205-975-9372; jakim@uab.edu.

Author Contributions

J.K. devised and coordinated the project. P.H., H.J., B.B. synthesized the nanomatrix gel. G.R., P.H., J.S., T.G. performed experiments. P.H., H.J., J.K., M.Y., B.B., T.G., C.P., S.B. provided expertise and wrote manuscript.

Disclosure/conflict of interest

Patrick Hwang, Reid Millican, Brigitta Brott, and Ho-Wook Jun are employees of Endomimetics, LLC. The remaining authors have no competing interests.

rodents. NO stimulates metabolic rate by increasing mitochondrial biogenesis and brown fat activation. Therefore, we propose a novel technology of providing exogenous NO to improve metabolic rate and cognitive function by promoting the development of brown adipose tissue. In the present study, we demonstrate the effects of the peptide amphiphiles-NO-releasing nanomatrix gel (PANO gel) in high-fat diet (HFD)-induced obesity, insulin resistance, and cognitive functions. Eight-week-old male C57BL/6 mice were subcutaneously injected in the brown fat area with the PANO gel or vehicle (PA gel) every two weeks for 12 weeks. The PANO gel-injected mice gained less body weight, improved glucose tolerance, and decreased fasting serum insulin and leptin levels compared with the PA gel-injected mice. Insulin signaling in muscle, liver and epididymal white adipose tissue (eWAT) was improved by the PANO gel injection. The PANO gel reduced inflammation, increased lipolysis in the eWAT, decreased serum lipids, and liver triglycerides. Interestingly, the PANO gel stimulated uncoupled protein 1 gene expression in the brown and beige fat tissues. Furthermore, the PANO gel increased cerebral blood flow and improved learning and memory abilities. Our results suggest that using the PANO gel to supply exogenous NO is a novel technology to treat metabolic disorders and cognitive dysfunctions.

Keywords

Nitric oxide; Nanomatrix; Inflammation; Obesity; Insulin resistance

INTRODUCTION

Obesity is a risk factor for various health problems, including hypertension, stroke, coronary artery disease, and type 2 diabetes (T2D)[1]. These abnormalities significantly increase cardiovascular events, cognitive decline, and mortality[2, 3]. There are prescription medications for lowering body weight. However, the benefits of weight control medications are limited as they remain less effective for obesity-associated cardiovascular disease and dementia[4–7]. Populations of obese and overweight subjects are increasing, and the mortality rate related to obesity is being elevated. Obesity is associated with reduced production of NO, mainly due to the decreased activity of endothelial nitric oxide synthase (eNOS). Reducing fat mass is accomplished by eating less (diet), decreasing appetite (most of the current pharmacological therapies), surgical procedures (bariatric surgery), or increasing energy expenditure (exercise). However, these approaches have weaknesses, including limited effectiveness, high cost, high reversion rates, and adherence to the healthy life-style is difficult. Thus, a novel strategy to treat obesity may help improve public health and slow the aging process.

Brown fat is characterized by high mitochondrial content and multilocular lipid droplets, facilitating fat oxidation and generating heat. Increasing brown fat elevates metabolic rate and reduces the risk of metabolic disorders[8, 9]. The existence of brown fat in humans was previously in doubt, but recent reports demonstrate that human brown fat does exist in the supraclavicular region[10]. Moreover, brown-like adipocytes have been found in white adipose tissue by conversion of white adipocytes to brown adipocyte-like cells (“beiging”) both in mice and humans[11]. The loss of brown fat is known to cause attenuation of metabolic rate and progressive development of obesity, insulin resistance, and T2D in humans[12].

Thus, the increasing brown and/or beige fat content may be a way to prevent and treat obesity-associated metabolic diseases.

Nitric oxide (NO) promotes the differentiation of white adipose tissue (WAT) to brown adipose tissue (BAT)[13], and endothelial nitric oxide synthase (eNOS) knockout mice have defective fat oxidation, hypertension, dyslipidemia, and insulin resistance that are also associated with aging[14, 15]. Reduced NO bioavailability is mainly due to the reduced eNOS activity[13, 16, 17] and increased oxidative stress[18, 19], which affects various metabolic processes, including mitochondrial biogenesis, glucose and fatty acid uptake, lipolysis, and brown adipocyte development[20]. Overexpression of eNOS decreases diet-induced obesity[16], and supplementation of L-arginine (elevation of NO production) increases the development of BAT[21]. Thus, increasing bioavailability of NO has beneficial effects on metabolism and related cardiovascular complications.

We have developed a peptide amphiphiles nanomatrix gel that releases sustained levels of NO (PANO gel) for a month, and we previously demonstrated that the PANO gel enhances angiogenesis and suppresses inflammatory responses[22–24]. The nanomatrix gel is composed of peptide amphiphiles (PAs), comprising multilayers of hydrophilic NO-releasing peptide sequences conjugated to hydrophobic alkyl tails. This amphiphilic property of PAs promotes the self-assembly of PAs into cylindrical micelle nanofibers that form a nanomatrix gel through cross-linking by the addition of calcium ions[23, 25]. The unique multilayered cylindrical micelle nanofibers with NO-releasing peptide enable generating NO[23–26]. The goal of the present study is to evaluate the effects of exogenous NO by the PANO gel on BAT on subsequent beneficial effects, such as weight loss, insulin sensitivity, and cognitive function.

MATERIALS AND METHODS

Production of NO-releasing nanomatrix gel

The peptides composed of a matrix metalloproteinase-2 (MMP-2) enzyme-mediated degradation site with a cell-adhesive sequence (YIGSR) or a NO reactive sequence (KKKKK) were alkylated with palmitic acid, which produced PA-YIGSR or PA-KKKKK, respectively. PA-YIGSR and PA-KKKKK were mixed at a 9:1 ratio (PA-YK) and then incubated with NO gas overnight (PA-YK-NO). PA-YK or PA-YK-NO was mixed with $CaCl_2$ (20 ul of 0.1M) to produce nanomatrix gel, as described previously[22, 25, 26]. The PA-YK-NO gel (PANO gel) was used to provide exogenous NO, and the PA-YK gel (PA gel) was used as a control (vehicle, V).

Animal housing and maintenance

All animal procedures were performed in accordance with the rules of and approved by the Animal Use and Care Committee at The University of Alabama at Birmingham. The six-week-old male C57BL/6J mice were purchased from The Jackson Laboratory (Bar Harbor, ME). All animals were maintained in a temperature-controlled facility with a 12:12-h light-dark cycle. Mice were fed a normal chow diet until the age of 8 weeks and then fed a high-fat-diet (HFD, 60% calories from fat, D13021802, Research Diets Inc., New

Brunswick, NJ). The mice were divided into two groups and were subcutaneously injected with either vehicle (PA gel, 50 μl) or nitric oxide (NO) releasing nanomatrix gel (PANO gel, 50 μl) biweekly.

Body composition measurement

These experiments were performed as previously described[27], and were conducted by the UAB small animal phenotyping core facility funded by the UAB *Nutrition Obesity Research Center*.

Glucose tolerance test and insulin tolerance test

Intraperitoneal glucose tolerance test (GTT) and insulin tolerance test (ITT) were performed after a 6 hr fast. During GTT, tail-vein blood glucose level was determined at 0, 15, 30, 60, and 120 min after intraperitoneal injection of 2g/kg body weight glucose with a hand-held glucometer (Freestyle; Abbott, Abbott Park, IL). Similarly, for the ITT, glucose levels were determined at 0, 15, 30, 60, and 90 min after intraperitoneal injection of 0.5 U/kg body weight insulin.

Measurement of serum parameters

The blood was collected from mice after a 6hr fast. The serum was collected of clotted blood after centrifugation at 2,200 g for 10 min at 4°C. Serum insulin levels were assessed by an ultrasensitive mouse insulin Enzyme-Linked Immunosorbent Assay (ELISA, Chrystal Chem, IL). Triglyceride levels were assessed using Pointe Scientific triglycerides liquid reagents (Pittsburgh, PA). Cholesterol levels were assessed using Thermo Scientific total cholesterol reagents (Pittsburgh, PA). Homeostatic Model Assessment of Insulin Resistance (HOMA-IR) was calculated as previously described[27].

Preparation of tissue lysates and immunoblotting

Insulin (1 U/kg) was injected intraperitoneally after a 6hr fast. Skeletal muscle, liver, and epididymal adipose tissue were collected and frozen in liquid nitrogen until used. Tissue homogenates were prepared according to the manufacturer's instruction for a Tissuelyser II (Qiagen, MD). Cell lysates were subjected to immunoblotting with antibodies as described previously[28], and the total protein as a loading control was visualized with a TGX stain-free imaging technology (Bio-Rad). Gel images were visualized and were quantified using ChemiDoc imaging system and Image Lab 5.0 software (Bio-Rad Laboratories).

Immunohistochemistry

The harvested tissues were fixed in 10% formaldehyde/PBS solution overnight. Paraffin blocks were prepared, and the tissue sections were processed as described elsewhere[27]. After the sections were blocked with ABC blocking serum (cat# PK-6105, Vector laboratories, Burlingame, CA) for 1 h, they were incubated overnight with an anti-F4/80 antibody (cat# 565409, BD Biosciences, San Diego CA) or anti-uncoupled protein 1 (UCP1) antibody (cat# ab10983, Abcam, Cambridge MA). The tissue sections were processed by using a Vectastain Elite ABC kit (Vector Laboratories, Burlingame, CA) according to the manufacturer's

instruction. In some cases, the tissue sections were stained with hematoxylin and eosin and mounted with permount. The slides were photographed and analyzed by light microscopy.

Quantitative real-time qPCR

Tissues were collected by snap-freezing in liquid nitrogen and then stored at −80 °C until analysis. Total RNA preparation, cDNA synthesis and qPCR were performed as previously published[27]. The primer sequences for the gene expression are; *Cyclophilin* F- CAGACGCCACTGTCGCTTT, R-TGTCTTTGGAACTTTGTCTG, *F4/80* F- TGCCACAACACTCTCGGAAGCTAT, R-TCCTGGAGCACTCATCCACATCTT; *Tnfa* F- CCAACGGCATGGATCTCAAAGACA, R-AGATAGCAAATCGGCTGACGGTGT; *CD68* F-CCCACCTGTCTCTCTCATTTC, R-GTATTCCACCGCCATGTAGT; *IL-1β* F-, CTCGCAGCAGCACATCAAC, R-ACGGGAAAGACACAGGTAGC; *Ucp1* F-AGGCTTCCAGTACCATTAGGT, R- CTGAGTGAGGCAAAGCTGATTT.

Cerebral blood flow measurement

Cerebral blood flow (CBF) was measured using a Laser Speckle Contrast Imager (LSCI) (Moor Instruments). CBF measurements were performed under anesthesia with 2% isoflurane. CBF values were assessed using regions of interest (ROIs) on both sides of the middle cerebral artery (MCA) areas on the lateral aspect of the brain. The images were recorded while the body temperature, heart rate and SPO_2 % were stably maintained for 1.5 min. The mean values from the 24 perfusion images were chosen for the quantification. The flux values were determined with the sum of the 6 different regions that did not include the MCA and were normalized with the values of the blood flow into the MCA region. Fluxes in the ROIs were expressed as arbitrary units using a 256-color palette.

Morris water maze

The water maze apparatus and procedure were performed as previously described[29]. Learning of the task was evaluated by recording the swimming speed, latency to find the platform, path length and percentage of trials for each animal that found the platform. After the end of the three trials on day 5 of the testing period, the mice were tested in a 60 s probe trial (i.e., trial 16), with no escape platform present.

Statistical analysis

Values were presented as mean ± standard error of the mean (SEM). Statistical significance between the two groups was assessed by a two-tailed Student's t-test with p-value less than 0.05. Statistical analysis for the water maze test was performed by two-way repeated measures ANOVA combined with Bonferroni post-doc test. Statistical analyses were performed using GraphPad Prism Version 9 (GraphPad Inc., San Diego, CA).

RESULTS

Nitric oxide-releasing nanomatrix gel and the time schedule of the animal experiment –

PANO gel has a self-assembly domain, bio-degradable site, and NO-releasing domain (Fig. 1A)[30]. To examine whether the elevated level of NO ameliorates HFD-induced

metabolic syndrome, eight-week-old male C57BL6/J mice were fed a HFD. The mice were subcutaneously injected with vehicle or the PANO gel every two weeks at the time of HFD feeding for 12 weeks (Fig. 1A). The PANO gel increased the phosphorylation of vasodilator-stimulated phosphor-protein (VASP) at Serine 239 amino acid residue (S^{239}) (Fig. 1B). pVASP (S^{239}), a marker for the stimulation of NO/cGMP/PKG pathway, is a substrate for cGMP-dependent kinase (PKG)[31]. The result suggests that the administration of the PANO gel stimulates the NO/cGMP/PKG pathway.

Mice injected with the PANO gel gained less body weight by reducing fat mass -

To examine whether the PANO gel affects HFD-induced weight gain, body weight was monitored weekly. The PANO gel-injected mice gained 16.8% less body weight compared with the vehicle-injected mice (39.3 g vs. 47.3 g) (Fig. 2A & 2B). To assess the difference in fat and lean masses, the body composition of mice was evaluated by a quantitative magnetic resonance (QMR). The reduction of body weight by the PANO gel was mainly by decreasing fat but not lean mass or water content (Fig. 2C). The reduced fat mass was visualized by the photos (Fig. 2A) and the weights of eWAT (Fig. 2D), inguinal adipose tissue (iWAT) (Fig. 2E), and BAT (Fig. 2F). The color of BAT was darker in the PANO gel-injected mice compared with the PA gel-injected mice.

Administration of the PANO gel reduced pro-inflammatory response and increased lipolysis in white adipose tissue.

Hypertrophied adipocytes are the prominent feature of obesity, and a chronic inflammatory response in WAT is associated with insulin resistance[32]. The size of adipocytes in the eWAT was reduced by the PANO gel (Fig. 3A, upper panel). The number of F4/80-positive, a macrophage maker, cells was smaller in the PANO gel-injected mice than in the vehicle-injected mice (Fig. 3A, lower panel). To confirm the result, the expression of pro-inflammatory genes in the eWAT was evaluated. Administration of the PANO gel reduced the expression of pro-inflammatory genes, including *F4/80, Il-1β, Tnfα*, and *Cd68* (Fig. 3B). The NO/cGMP/PKG pathway stimulates lipolysis[17]. Therefore, we examined whether the PANO gel stimulates the phosphorylation of hormone sensitive lipase (HSL), a key enzyme for lipolysis. Administration of the PANO gel increased the phosphorylation of HSL in eWAT (Fig. 3C). These results suggest that the PANO gel potentially decreases HFD-induced weight gain by increasing the lipolysis in eWAT.

The PANO gel increased UCP1 expression in BAT and iWAT -

NO stimulates brown adipose tissue by mitochondrial biogenesis[33]. We examined whether administration of exogenous NO can stimulate BAT and browning of WAT. Consistent with the results in Fig 3, the sizes of adipocytes in BAT and iWAT are smaller in the PANO gel-injected mice than those in the vehicle-injected mice (Fig. 4A). Also the gene expression of browning gene, *Ucp1* was elevated in the BAT and the iWAT by the PANO gel injection (Fig. 4A). Furthermore, the protein levels of UCP1 in the BAT and the iWAT were higher in the PANO gel-injected mice than in vehicle-injected mice (Fig. 4B). These results suggest that the PANO gel stimulates the browning of adipose tissue.

The PANO gel protected from HFD-induced nonalcoholic fatty liver -

HFD causes the accumulation of lipids in the liver, and obesity is associated with nonalcoholic fatty liver disease[34, 35]. The administration of the PANO gel reduced the accumulation of lipids in the liver (Fig. 5A & 5B). This result was confirmed by the reduced liver weight and the triglyceride (TG) contents in the liver (Fig. 5C & 5D). The circulating TG and cholesterol levels were lower in the PANO gel-injected mice (Fig. 5E & 5F).

The PANO gel improved insulin sensitivity –

Obesity is associated with type 2 diabetes, including insulin resistance and glucose intolerance. Insulin resistance and cardiometabolic syndrome are caused by impaired NO production[36]. We examined the effects of exogenous administration of the PANO gel on glucose homeostasis and insulin sensitivity. The PANO gel-injected group demonstrated improved glucose and insulin tolerance (Fig. 6A & 6B). Furthermore, fasting glucose and insulin levels were decreased by the PANO gel injection (Fig. 6C & 6D). The index for insulin sensitivity, HOMA-IR, indicated that the PANO gel improved insulin sensitivity (Fig. 6E). To examine whether the PANO gel improves insulin signaling pathways, cell lysates from the major metabolic tissues, skeletal muscle, liver, and adipose tissue, were subjected to western blots with antibodies for insulin signaling molecules. Insulin-stimulated phosphorylation of insulin signaling molecules was enhanced in skeletal muscle (Fig. 7A - 7E), liver (Fig. 7F -7J), and eWAT (Fig. 7K - 7N). These results suggest that the PANO gel improved insulin sensitivity and insulin actions in metabolic tissues.

The PANO gel improved cerebral blood flow (CBF) and cognitive function –

Injection of the PANO gel increased the cerebral blood flow while stably maintaining the body temperature, heart rate, and blood pressure (Fig. 8A – 8E). Because HFD reduces cerebral blood flow and leads to decreased cognitive function[37], we examined the consequence of the improved CBF by assessing spatial learning ability with the Morris water maze test. We observed that the PANO gel significantly improved spatial learning ability (Fig. 8F).

DISCUSSION

The present study demonstrates that subcutaneous injection of the NO-releasing nanomatrix gel (PANO gel) ameliorates HFD-induced metabolic and cognitive dysfunctions, including weight gain, fatty liver, and chronic inflammation in WAT, hyperlipidemia, glucose intolerance, insulin resistance, and spatial learning deficits. The metabolic effects of the PANO gel seem to be due to increased lipolysis and browning of WAT (Fig. 3 & 4). The strategy of reducing body weight by the local delivery of NO may be a novel, efficient, and safe way to prevent and treat multiple metabolic diseases.

Despite its short half-life, NO has essential biological roles in vasodilation, mitochondrial biogenesis, anti-inflammation, and glucose uptake[33, 38–40]. The decreased NO bioavailability is associated with aging and cardiometabolic syndrome, including insulin resistance, diabetes, atherosclerosis, heart failure, and dementia[36, 41–43]. There have been various efforts to supplement exogenous NO-related agents, including L-arginine,

NO inhalation, and other NO donors, and phosphodiesterase-5 (PDE-5) inhibitors[44]. Supplementing exogenous NO improves cardiovascular and neuronal function[42, 43, 45–47]. Although the previously reported reagents have some positive effects, most of the reagents are used for acute injuries, including stroke, hemorrhage, trauma and encephalopathy[44]. PDE-5 inhibitors have vasodilatory effects and reduce the damage from cerebral infarction and hemorrhage[48], but other study shows no effect on brain perfusion[49]. Sildenafil improves metabolic functions but has some inconclusive effects on cerebral blood flow[48–51]. Furthermore, L-arginine reduces body weight and improves glucose intolerance[21, 52]. However, a few clinical studies show that the effect of L-arginine is elusive[53, 54]. Thus, developing a novel strategy to provide sustained levels of exogenous NO will be an efficient way of treating cardiometabolic disorders. We have developed a novel nanomatrix gel that releases NO[22, 23]. The PANO gel has the following characteristics; 1) sustained release of NO over 30 days, 2) promotion of angiogenesis, 3) NO release to promote blood vessel dilation and suppresses inflammatory responses, and 4) a biocompatible peptide-based material[22, 23, 26, 55]. These unique characteristics of the PANO gel enable the amelioration of chronic diseases, such as metabolic and cognitive dysfunctions. NO-stimulated cGMP increases the phosphorylation of HSL and lipolysis through a cGMP-cGMP-dependent kinase 1 (cGKI)-dependent mechanism in adipocytes[56]. Thus, the increased lipolysis may explain the reduced body weight and fat mass. Furthermore, NO/cGMP pathway stimulates the peroxisome proliferator-activated receptor-gamma coactivator-1α (PGC-1α), which stimulates the expression of nuclear respiratory factor 1 (NRF-1), and mitochondrial transcription factor A (mtTFA). These transcription factors regulate the gene expression of mitochondrial genes, such as cytochrome c and cyclooxygenase IV[33]. The increased mitochondrial biogenesis is one of the mechanisms for the conversion of white adipocytes to beige adipocytes[57, 58]. The adipose tissue beiging reduces weight gain and fatty acid utilization[57, 58]. The effect of the PANO gel on adipose tissue beiging may contribute to glucose homeostasis and insulin sensitivity. Likewise, we observed that the PANO gel improves glucose tolerance and insulin sensitivity (Fig. 6 & 7). Moreover, the vasodilatory effect of NO results in increased blood flow and capillary recruitment, which facilitates glucose uptake in skeletal muscle[59]. The vascular action on glucose uptake is dependent on insulin activating insulin receptor/insulin receptor substrates1 and 2/phosphoinositide-dependent kinase 1 (PDK1)/Akt/eNOS pathway[60, 61]. The effect of the PANO gel on glucose uptake mimics the insulin signaling pathway that has been suggested for treating cardiometabolic syndrome[62]. Although improving endothelial function by diet and exercise can elevate the physiological level of NO[63], pharmacological approaches to increase NO are useful strategies to treat diseases in clinical settings. NO inhalation and direct NO donors, such as sodium nitroprusside, nitroglycerin, and nitrates are used for angina, heart failure, pulmonary hypertension, and erectile dysfunction[64]. However, long-term usage is not recommended because of the safety issues, such as hypotension and other side effects of hypernitrosylation[65]. Thus, the usage of these reagents for metabolic disorders is limited. The effects of phosphodiesterase-5 (PDE-5) inhibitors, such as sildenafil or vardenafil, on the beneficial metabolic effects in addition to erectile dysfunction and cardiovascular disorders have been evaluated[51, 66]. The combination therapy of leucine, metformin, and sildenafil has a weight loss effect and improves insulin sensitivity and non-alcoholic fatty liver disease[66, 67]. On the other hand, sildenafil alone does not have a weight loss effect

although browning of WAT was observed[50]. Also, the intake of L-arginine, which is the substrate of nitric oxide synthase, improves insulin sensitivity and reduces body weight when hypocaloric diet and exercise are combined[68, 69]. This suggests that none of the currently available therapies provide all the benefits delivered by monotherapy with the PANO gel on weight loss, glucose homeostasis, and insulin resistance. Thus, the PANO gel alone may be a novel monotherapy approach to improve metabolic functions.

HFD causes cerebrovascular dysfunction associated with cognitive impairment and dementia[37]. Beige adipocytes mediate neuroprotective and anti-inflammatory effects[70]. At present, it is unknown whether our observed effects of the PANO gel on cerebrovascular blood flow and cognitive function are the direct effect of NO or are mediated by the neuroprotective effects of the adipocyte beiging[70].

Although the PANO gel releases NO for up to a month[24], we applied the PANO gel biweekly. The tissue level of NO released from PANO gel may be determined by multiple factors, including the injection volume and frequency, injection tissue, and body weight. We empirically determined the injection volume and the frequency of PANO gel by monitoring the effects on gaining less weight. Thus, the dose and the frequency of PANO gel in future clinical studies may also require optimizing the dose and the injection frequency.

CONCLUSIONS

The PANO gel reduces the HFD-induced weight gain, fatty liver, and pro-inflammatory response while increasing glucose tolerance and insulin sensitivity. Activation of beige adipose tissue increases fatty acid oxidation and energy expenditure, which enhances metabolic rate. Because reduced bioavailability of NO is the hallmark of cardiometabolic syndrome, supplying exogenous NO at a sustained level may be an efficient way of treating the cardiometabolic syndrome. We conclude that our technology is a novel strategy to improve metabolic and cognitive function.

Acknowledgments

This study was supported by the UAB Diabetes Research Center sponsored pilot and feasibility program supported by the National Institutes of Health (P30DK079626), and UAB Comprehensive Diabetes Center and National Heart Lung and Blood Institute (R01 HL128695 to JK and R01HL163802 to HJ) National Institute of Aging (R03 AG058078 to JK), National Institute of Diabetes and Digestive and Kidney NIH-NIDDK (R00 DK95975-03 and 1R01DK120684-01 to SB, R44DK109789 to PH). Behavioral studies were supported by the UAB Neuroscience Behavioral Assessment Core (funded by P30NS047466)

Data and Resource Availability

All primary data and animal models used in the study are available to investigators upon reasonable request.

REFERENCES

1. Despres JP; Lemieux I; Bergeron J; Pibarot P; Mathieu P; Larose E; Rodes-Cabau J; Bertrand OF; Poirier P, Abdominal Obesity and the Metabolic Syndrome: Contribution to Global Cardiometabolic Risk. Arterioscler Thromb Vasc Biol 2008, 28 (6), 1039–49. [PubMed: 18356555]

2. Brostow DP; Hirsch AT; Collins TC; Kurzer MS, The Role of Nutrition and Body Composition in Peripheral Arterial Disease. Nat Rev Cardiol 2012, 9 (11), 634–43. [PubMed: 22922595]

3. Tanaka H; Gourley DD; Dekhtyar M; Haley AP, Cognition, Brain Structure, and Brain Function in Individuals with Obesity and Related Disorders. Curr Obes Rep 2020.

4. Merx MW; Liehn EA; Janssens U; Lutticken R; Schrader J; Hanrath P; Weber C, Hmg-Coa Reductase Inhibitor Simvastatin Profoundly Improves Survival in a Murine Model of Sepsis. Circulation 2004, 109 (21), 2560–5. [PubMed: 15123521]

5. Koh KK; Han SH; Quon MJ; Yeal Ahn J; Shin EK, Beneficial Effects of Fenofibrate to Improve Endothelial Dysfunction and Raise Adiponectin Levels in Patients with Primary Hypertriglyceridemia. Diabetes Care 2005, 28 (6), 1419–24. [PubMed: 15920062]

6. Barrea L; Pugliese G; Muscogiuri G; Laudisio D; Colao A; Savastano S, New-Generation Anti-Obesity Drugs: Naltrexone/Bupropion and Liraglutide. An Update for Endocrinologists and Nutritionists. Minerva Endocrinol 2020, 45 (2), 127–137. [PubMed: 32643356]

7. Srivastava G; Apovian C, Future Pharmacotherapy for Obesity: New Anti-Obesity Drugs on the Horizon. Curr Obes Rep 2018, 7 (2), 147–161. [PubMed: 29504049]

8. Poher AL; Altirriba J; Veyrat-Durebex C; Rohner-Jeanrenaud F, Brown Adipose Tissue Activity as a Target for the Treatment of Obesity/Insulin Resistance. Front Physiol 2015, 6, 4. [PubMed: 25688211]

9. Virtanen KA, Bat Thermogenesis: Linking Shivering to Exercise. Cell Metab 2014, 19 (3), 352–4. [PubMed: 24606895]

10. Hu HH, Magnetic Resonance of Brown Adipose Tissue: A Review of Current Techniques. Crit Rev Biomed Eng 2015, 43 (2–3), 161–81. [PubMed: 27278740]

11. Enerback S, Adipose Tissue Metabolism in 2012: Adipose Tissue Plasticity and New Therapeutic Targets. Nat Rev Endocrinol 2013, 9 (2), 69–70. [PubMed: 23296169]

12. Rogers NH; Landa A; Park S; Smith RG, Aging Leads to a Programmed Loss of Brown Adipocytes in Murine Subcutaneous White Adipose Tissue. Aging Cell 2012, 11 (6), 1074–83. [PubMed: 23020201]

13. Nisoli E; Clementi E; Tonello C; Sciorati C; Briscini L; Carruba MO, Effects of Nitric Oxide on Proliferation and Differentiation of Rat Brown Adipocytes in Primary Cultures. Br J Pharmacol 1998, 125 (4), 888–94. [PubMed: 9831929]

14. Duplain H; Burcelin R; Sartori C; Cook S; Egli M; Lepori M; Vollenweider P; Pedrazzini T; Nicod P; Thorens B; Scherrer U, Insulin Resistance, Hyperlipidemia, and Hypertension in Mice Lacking Endothelial Nitric Oxide Synthase. Circulation 2001, 104 (3), 342–5. [PubMed: 11457755]

15. Le Gouill E; Jimenez M; Binnert C; Jayet PY; Thalmann S; Nicod P; Scherrer U; Vollenweider P, Endothelial Nitric Oxide Synthase (Enos) Knockout Mice Have Defective Mitochondrial Beta-Oxidation. Diabetes 2007, 56 (11), 2690–6. [PubMed: 17682093]

16. Sansbury BE; Cummins TD; Tang Y; Hellmann J; Holden CR; Harbeson MA; Chen Y; Patel RP; Spite M; Bhatnagar A; Hill BG, Overexpression of Endothelial Nitric Oxide Synthase Prevents Diet-Induced Obesity and Regulates Adipocyte Phenotype. Circ Res 2012, 111 (9), 1176–89. [PubMed: 22896587]

17. Elizalde M; Ryden M; van Harmelen V; Eneroth P; Gyllenhammar H; Holm C; Ramel S; Olund A; Arner P; Andersson K, Expression of Nitric Oxide Synthases in Subcutaneous Adipose Tissue of Nonobese and Obese Humans. J Lipid Res 2000, 41 (8), 1244–51. [PubMed: 10946012]

18. Munzel T; Daiber A; Ullrich V; Mulsch A, Vascular Consequences of Endothelial Nitric Oxide Synthase Uncoupling for the Activity and Expression of the Soluble Guanylyl Cyclase and the Cgmp-Dependent Protein Kinase. Arterioscler Thromb Vasc Biol 2005, 25 (8), 1551–7. [PubMed: 15879305]

19. Paxinou E; Weisse M; Chen Q; Souza JM; Hertkorn C; Selak M; Daikhin E; Yudkoff M; Sowa G; Sessa WC; Ischiropoulos H, Dynamic Regulation of Metabolism and Respiration by Endogenously Produced Nitric Oxide Protects against Oxidative Stress. Proc Natl Acad Sci U S A 2001, 98 (20), 11575–80. [PubMed: 11562476]

20. Dai Z; Wu Z; Yang Y; Wang J; Satterfield MC; Meininger CJ; Bazer FW; Wu G, Nitric Oxide and Energy Metabolism in Mammals. Biofactors 2013, 39 (4), 383–91. [PubMed: 23553707]

21. Wu Z; Satterfield MC; Bazer FW; Wu G, Regulation of Brown Adipose Tissue Development and White Fat Reduction by L-Arginine. Curr Opin Clin Nutr Metab Care 2012, 15 (6), 529–38. [PubMed: 23075933]

22. Andukuri A; Sohn YD; Anakwenze CP; Lim DJ; Brott BC; Yoon YS; Jun HW, Enhanced Human Endothelial Progenitor Cell Adhesion and Differentiation by a Bioinspired Multifunctional Nanomatrix. Tissue Eng Part C Methods 2013, 19 (5), 375–85. [PubMed: 23126402]

23. Alexander GC; Vines JB; Hwang P; Kim T; Kim JA; Brott BC; Yoon YS; Jun HW, Novel Multifunctional Nanomatrix Reduces Inflammation in Dynamic Conditions in Vitro and Dilates Arteries Ex Vivo. ACS Appl Mater Interfaces 2016, 8 (8), 5178–87. [PubMed: 26849167]

24. Somarathna M; Hwang PT; Millican RC; Alexander GC; Isayeva-Waldrop T; Sherwood JA; Brott BC; Falzon I; Northrup H; Shiu YT; Stubben CJ; Totenhagen J; Jun HW; Lee T, Nitric Oxide Releasing Nanomatrix Gel Treatment Inhibits Venous Intimal Hyperplasia and Improves Vascular Remodeling in a Rodent Arteriovenous Fistula. Biomaterials 2021, 121254. [PubMed: 34836683]

25. Anderson JM; Andukuri A; Lim D; Jun HW, Modulating the Gelation Properties of Self-Assembling Peptide Amphiphiles. ACS Nano 2009, 9, 3447–3454.

26. Kushwaha M; Anderson J; Minor W; Andukuri A; Bosworth C; Lancaster J; Brott B; Anderson P; Jun HW, Native Endothelium Mimicking Self-Assembled Nanomatrix for Cardiovascular Devices. Biomaterials 2010, 31, 1502–1508. [PubMed: 19913295]

27. Ren G; Kim T; Kim HS; Young ME; Muccio DD; Atigadda VR; Blum SI; Tse HM; Habegger KM; Bhatnagar S; Coric T; Bjornsti MA; Shalev A; Frank SJ; Kim JA, A Small Molecule, Uab126, Reverses Diet-Induced Obesity and Its Associated Metabolic Disorders. Diabetes 2020, 69 (9), 2003–2016. [PubMed: 32611548]

28. Kim HS; Montana V; Jang HJ; Parpura V; Kim JA, Epigallocatechin Gallate (Egcg) Stimulates Autophagy in Vascular Endothelial Cells: A Potential Role for Reducing Lipid Accumulation. J Biol Chem 2013, 288 (31), 22693–705. [PubMed: 23754277]

29. Liu L; Ikonen S; Heikkinen T; Tapiola T; van Groen T; Tanila H, The Effects of Long-Term Treatment with Metrifonate, a Cholinesterase Inhibitor, on Cholinergic Activity, Amyloid Pathology, and Cognitive Function in App and Ps1 Doubly Transgenic Mice. Exp Neurol 2002, 173 (2), 196–204. [PubMed: 11822883]

30. Kushwaha M; Anderson J; Minor W; Andukuri A; Bosworth C; J. L. Jr; Brott B; Anderson P; Jun HW, Natural Endothelium Mimicking Self-Assembled Nanomatrix for Drug Eluting Stent Applications. Circulation 2008, 118, S962.

31. Oelze M; Mollnau H; Hoffmann N; Warnholtz A; Bodenschatz M; Smolenski A; Walter U; Skatchkov M; Meinertz T; Munzel T, Vasodilator-Stimulated Phosphoprotein Serine 239 Phosphorylation as a Sensitive Monitor of Defective Nitric Oxide/Cgmp Signaling and Endothelial Dysfunction. Circ Res 2000, 87 (11), 999–1005. [PubMed: 11090544]

32. Xu H; Barnes GT; Yang Q; Tan G; Yang D; Chou CJ; Sole J; Nichols A; Ross JS; Tartaglia LA; Chen H, Chronic Inflammation in Fat Plays a Crucial Role in the Development of Obesity-Related Insulin Resistance. J Clin Invest 2003, 112 (12), 1821–30. [PubMed: 14679177]

33. Nisoli E; Clementi E; Paolucci C; Cozzi V; Tonello C; Sciorati C; Bracale R; Valerio A; Francolini M; Moncada S; Carruba MO, Mitochondrial Biogenesis in Mammals: The Role of Endogenous Nitric Oxide. Science 2003, 299 (5608), 896–9. [PubMed: 12574632]

34. Cusi K, Role of Obesity and Lipotoxicity in the Development of Nonalcoholic Steatohepatitis: Pathophysiology and Clinical Implications. Gastroenterology 2012, 142 (4), 711–725 e6. [PubMed: 22326434]

35. Li J; Deng Q; Zhang Y; Wu D; Li G; Liu J; Zhang L; Wang HD, Three Novel Dietary Phenolic Compounds from Pickled Raphanus Sativus L. Inhibit Lipid Accumulation in Obese Mice by Modulating the Gut Microbiota Composition. Mol Nutr Food Res 2021, 65 (6), e2000780. [PubMed: 33560577]

36. Kim JA; Montagnani M; Koh KK; Quon MJ, Reciprocal Relationships between Insulin Resistance and Endothelial Dysfunction: Molecular and Pathophysiological Mechanisms. Circulation 2006, 113 (15), 1888–904. [PubMed: 16618833]

37. Zuloaga KL; Johnson LA; Roese NE; Marzulla T; Zhang W; Nie X; Alkayed FN; Hong C; Grafe MR; Pike MM; Raber J; Alkayed NJ, High Fat Diet-Induced Diabetes in Mice Exacerbates

Cognitive Deficit Due to Chronic Hypoperfusion. J Cereb Blood Flow Metab 2016, 36 (7), 1257–70. [PubMed: 26661233]

38. Scherrer U; Randin D; Vollenweider P; Vollenweider L; Nicod P, Nitric Oxide Release Accounts for Insulin's Vascular Effects in Humans. J Clin Invest 1994, 94 (6), 2511–5. [PubMed: 7989610]
39. Baron AD, The Coupling of Glucose Metabolism and Perfusion in Human Skeletal Muscle. The Potential Role of Endothelium-Derived Nitric Oxide. Diabetes 1996, 45 Suppl 1, S105–9.
40. Patel RP; Levonen A; Crawford JH; Darley-Usmar VM, Mechanisms of the Pro- and Anti-Oxidant Actions of Nitric Oxide in Atherosclerosis. Cardiovasc Res 2000, 47 (3), 465–74. [PubMed: 10963720]
41. Wilson AM; Harada R; Nair N; Balasubramanian N; Cooke JP, L-Arginine Supplementation in Peripheral Arterial Disease: No Benefit and Possible Harm. Circulation 2007, 116 (2), 188–95. [PubMed: 17592080]
42. Pastor P; Curvello V; Hekierski H; Armstead WM, Inhaled Nitric Oxide Protects Cerebral Autoregulation through Prevention of Impairment of Atp and Calcium Sensitive K Channel Mediated Cerebrovasodilation after Traumatic Brain Injury. Brain Res 2019, 1711, 1–6. [PubMed: 30629942]
43. Gori T, Exogenous No Therapy for the Treatment and Prevention of Atherosclerosis. Int J Mol Sci 2020, 21 (8).
44. Toda N; Ayajiki K; Okamura T, Cerebral Blood Flow Regulation by Nitric Oxide: Recent Advances. Pharmacol Rev 2009, 61 (1), 62–97. [PubMed: 19293146]
45. Lerman A; Burnett JC Jr.; Higano ST; McKinley LJ; Holmes DR Jr., Long-Term L-Arginine Supplementation Improves Small-Vessel Coronary Endothelial Function in Humans. Circulation 1998, 97 (21), 2123–8. [PubMed: 9626172]
46. Elrod JW; Greer JJ; Lefer DJ, Sildenafil-Mediated Acute Cardioprotection Is Independent of the No/Cgmp Pathway. Am J Physiol Heart Circ Physiol 2007, 292 (1), H342–7. [PubMed: 16951048]
47. Ferguson SK; Woessner MN; Holmes MJ; Belbis MD; Carlstrom M; Weitzberg E; Allen JD; Hirai DM, Effects of Inorganic Nitrate Supplementation on Cardiovascular Function and Exercise Tolerance in Heart Failure. J Appl Physiol (1985) 2021, 130 (4), 914–922. [PubMed: 33475460]
48. Sheng M; Lu H; Liu P; Li Y; Ravi H; Peng SL; Diaz-Arrastia R; Devous MD; Womack KB, Sildenafil Improves Vascular and Metabolic Function in Patients with Alzheimer's Disease. J Alzheimers Dis 2017, 60 (4), 1351–1364. [PubMed: 29036811]
49. Dhar R; Washington C; Diringer M; Zazulia A; Jafri H; Derdeyn C; Zipfel G, Acute Effect of Intravenous Sildenafil on Cerebral Blood Flow in Patients with Vasospasm after Subarachnoid Hemorrhage. Neurocrit Care 2016, 25 (2), 201–4. [PubMed: 26940913]
50. Li S; Li Y; Xiang L; Dong J; Liu M; Xiang G, Sildenafil Induces Browning of Subcutaneous White Adipose Tissue in Overweight Adults. Metabolism 2018, 78, 106–117. [PubMed: 28986166]
51. Rebello CJ; Zemel MB; Kolterman O; Fleming GA; Greenway FL, Leucine and Sildenafil Combination Therapy Reduces Body Weight and Metformin Enhances the Effect at Low Dose: A Randomized Controlled Trial. Am J Ther 2021, 28 (1), e1–e13. [PubMed: 33369909]
52. Tan B; Li X; Yin Y; Wu Z; Liu C; Tekwe CD; Wu G, Regulatory Roles for L-Arginine in Reducing White Adipose Tissue. Front Biosci (Landmark Ed) 2012, 17, 2237–46. [PubMed: 22652774]
53. Rashid J; Kumar SS; Job KM; Liu X; Fike CD; Sherwin CMT, Therapeutic Potential of Citrulline as an Arginine Supplement: A Clinical Pharmacology Review. Paediatr Drugs 2020, 22 (3), 279–293. [PubMed: 32140997]
54. Boger RH, L-Arginine Therapy in Cardiovascular Pathologies: Beneficial or Dangerous? Curr Opin Clin Nutr Metab Care 2008, 11 (1), 55–61. [PubMed: 18090660]
55. Andukuri A; Minor W; Kushwaha M; Anderson J; Jun HW, Effect of Endothelium Mimicking Self-Assembled Nanomatrices on Cell Adhesion and Spreading of Human Endothelial Cells and Smooth Muscle Cells. Nanomedicine 2010, 6, 289–297. [PubMed: 19800987]
56. Sengenes C; Bouloumie A; Hauner H; Berlan M; Busse R; Lafontan M; Galitzky J, Involvement of a Cgmp-Dependent Pathway in the Natriuretic Peptide-Mediated Hormone-Sensitive Lipase Phosphorylation in Human Adipocytes. J Biol Chem 2003, 278 (49), 48617–26. [PubMed: 12970365]

57. Barquissau V; Beuzelin D; Pisani DF; Beranger GE; Mairal A; Montagner A; Roussel B; Tavernier G; Marques MA; Moro C; Guillou H; Amri EZ; Langin D, White-to-Brite Conversion in Human Adipocytes Promotes Metabolic Reprogramming Towards Fatty Acid Anabolic and Catabolic Pathways. Mol Metab 2016, 5 (5), 352–65. [PubMed: 27110487]
58. Lee P; Werner CD; Kebebew E; Celi FS, Functional Thermogenic Beige Adipogenesis Is Inducible in Human Neck Fat. Int J Obes (Lond) 2014, 38 (2), 170–6. [PubMed: 23736373]
59. Baron AD; Tarshoby M; Hook G; Lazaridis EN; Cronin J; Johnson A; Steinberg HO, Interaction between Insulin Sensitivity and Muscle Perfusion on Glucose Uptake in Human Skeletal Muscle: Evidence for Capillary Recruitment. Diabetes 2000, 49 (5), 768–74. [PubMed: 10905485]
60. Montagnani M; Chen H; Barr VA; Quon MJ, Insulin-Stimulated Activation of Enos Is Independent of Ca2+ but Requires Phosphorylation by Akt at Ser(1179). J Biol Chem 2001, 276 (32), 30392–8. [PubMed: 11402048]
61. Montagnani M; Ravichandran LV; Chen H; Esposito DL; Quon MJ, Insulin Receptor Substrate-1 and Phosphoinositide-Dependent Kinase-1 Are Required for Insulin-Stimulated Production of Nitric Oxide in Endothelial Cells. Mol Endocrinol 2002, 16 (8), 1931–42. [PubMed: 12145346]
62. Levine AB; Punihaole D; Levine TB, Characterization of the Role of Nitric Oxide and Its Clinical Applications. Cardiology 2012, 122 (1), 55–68. [PubMed: 22722323]
63. Sessa WC; Pritchard K; Seyedi N; Wang J; Hintze TH, Chronic Exercise in Dogs Increases Coronary Vascular Nitric Oxide Production and Endothelial Cell Nitric Oxide Synthase Gene Expression. Circ Res 1994, 74 (2), 349–53. [PubMed: 7507417]
64. Oudot A; Behr-Roussel D; Le Coz O; Poirier S; Bernabe J; Alexandre L; Giuliano F, How Does Chronic Sildenafil Prevent Vascular Oxidative Stress in Insulin-Resistant Rats? J Sex Med 2010, 7 (1 Pt 1), 79–88. [PubMed: 19845545]
65. Yoon S; Eom GH; Kang G, Nitrosative Stress and Human Disease: Therapeutic Potential of Denitrosylation. Int J Mol Sci 2021, 22 (18).
66. Zemel MB; Kolterman O; Rinella M; Vuppalanchi R; Flores O; Barritt A. S. t.; Siddiqui M; Chalasani N, Randomized Controlled Trial of a Leucine-Metformin-Sildenafil Combination (Ns-0200) on Weight and Metabolic Parameters. Obesity (Silver Spring) 2019, 27 (1), 59–67. [PubMed: 30569637]
67. Bruckbauer A; Banerjee J; Fu L; Li F; Cao Q; Cui X; Wu R; Shi H; Xue B; Zemel MB, A Combination of Leucine, Metformin, and Sildenafil Treats Nonalcoholic Fatty Liver Disease and Steatohepatitis in Mice. Int J Hepatol 2016, 2016, 9185987. [PubMed: 28042486]
68. Hu S; Han M; Rezaei A; Li D; Wu G; Ma X, L-Arginine Modulates Glucose and Lipid Metabolism in Obesity and Diabetes. Curr Protein Pept Sci 2017, 18 (6), 599–608. [PubMed: 27356939]
69. Lucotti P; Setola E; Monti LD; Galluccio E; Costa S; Sandoli EP; Fermo I; Rabaiotti G; Gatti R; Piatti P, Beneficial Effects of a Long-Term Oral L-Arginine Treatment Added to a Hypocaloric Diet and Exercise Training Program in Obese, Insulin-Resistant Type 2 Diabetic Patients. Am J Physiol Endocrinol Metab 2006, 291 (5), E906–12. [PubMed: 16772327]
70. Guo DH; Yamamoto M; Hernandez CM; Khodadadi H; Baban B; Stranahan AM, Beige Adipocytes Mediate the Neuroprotective and Anti-Inflammatory Effects of Subcutaneous Fat in Obese Mice. Nat Commun 2021, 12 (1), 4623. [PubMed: 34330904]

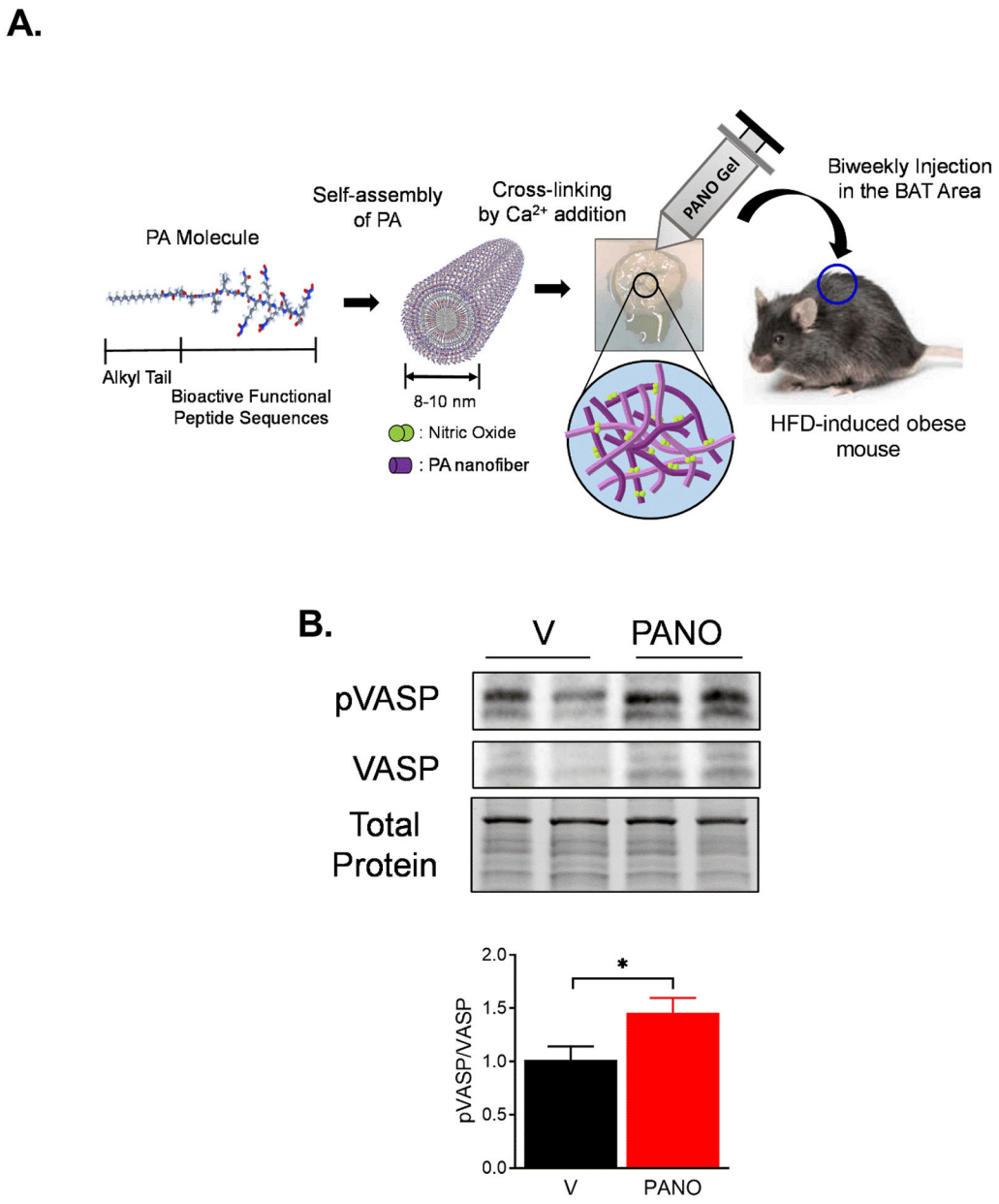

FIGURE 1. NO-releasing nanomatrix gel and the animal experiment schedule.

(A) Biocompatible PANO gel comprises an alkyl tail, MMP-2 degradable site, cell adhesion, and NO-releasing moieties. Eight-week-old male C57BL6/J mice were fed an HFD for 12 weeks. PANO gel or vehicle (PA, control gel without NO) was injected subcutaneously into the area where BAT is located biweekly. **(B)** BAT was isolated from mice, and the cell lysates were prepared. The cell lysate was subjected to a Western blotting with the indicated antibodies. NO level indicator, p-VASP, was increased by the PANO gel injection. Total protein as a loading control is shown with a stain-free gel. The blot is a representative gel. Data are presented as mean ± SEM (n=6). *p<0.05.

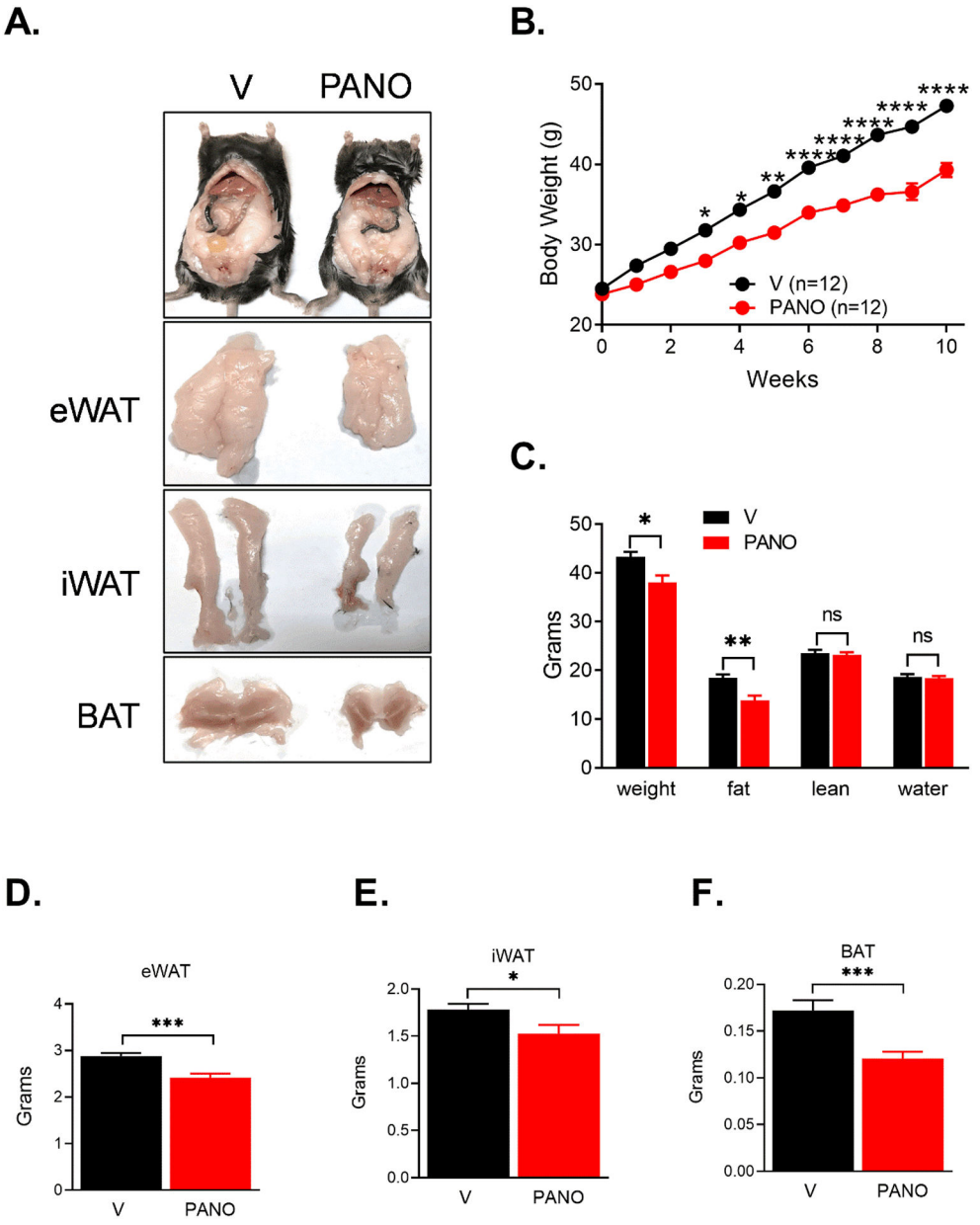

FIGURE 2. Mice injected with the PANO gel gained less body weight.

(A) Eight-week-old male mice were divided into two groups (12 mice/group) and injected with vehicle (V) or the PANO gel biweekly. **(B)** The body weight was monitored weekly. The PANO gel-injected mice gained less body weight. (n=12 – 13) Data are presented as mean ± SEM. *p<0.05, **p<0.01, ***p<0.001, and ****p<0.0001. **(C)** The mice were subjected to a quantitative magnetic resonance (QMR) analysis. Administration of the PANO gel reduced fat mass but not lean mass or water content. Data are presented as mean ± SEM (n=6). *p<0.05, **p<0.01, and n.s. not significant. Adipose tissues were isolated and weighed. **(D)** Administration of the PANO gel reduced the weight of adipose tissue. Epididymal adipose tissue (eWAT), **(E)** inguinal adipose tissue (iWAT), and **(F)**

brown adipose tissue (BAT). Data are presented as mean ± SEM (n= 18 – 19). *p<0.05 and ***p<0.001.

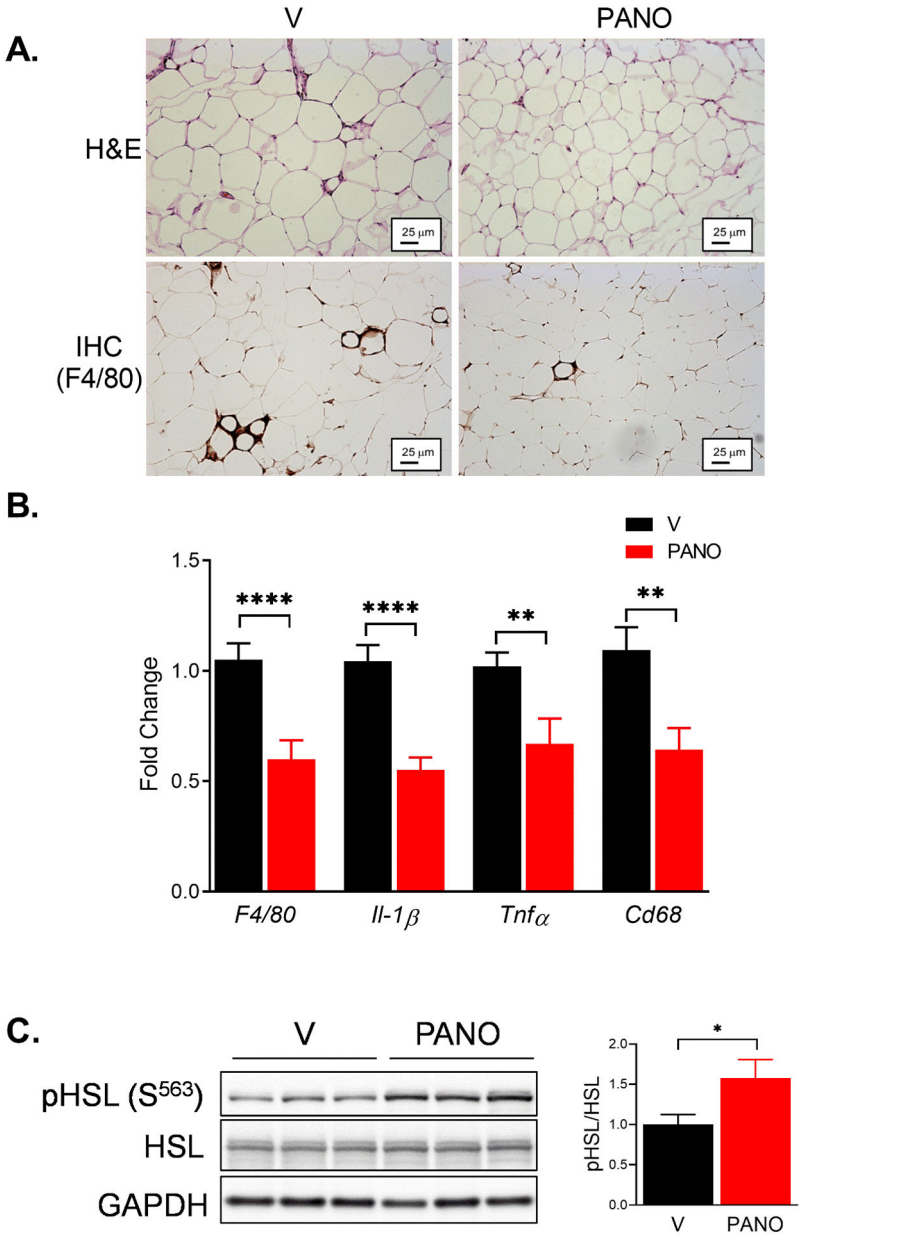

FIGURE 3. Administration of the PANO gel reduced pro-inflammatory response and increases lipolysis in white adipose tissue.

Male epididymal fat was isolated from HFD-fed mice injected with V or the PANO gel. **(A)** H & E staining (upper panel) and immunohistochemistry with anti-F4/80 antibody (lower panel) on eWAT were performed. Adipocyte size and F4/80 positive cells were reduced by the PANO gel injection. **(B)** mRNA was isolated from eWAT and the inflammatory gene expression was evaluated. The pro-inflammatory response was reduced by the PANO gel injection. Data are presented as mean ± SEM (n=6). **p<0.01 and ****p<0.0001 (n = 9–12). **(C)** Western blots on the lysate isolated from eWAT. pHSL was increased in the PANO gel injected mice. Data are presented as mean ± SEM (n=12). *p<0.05.

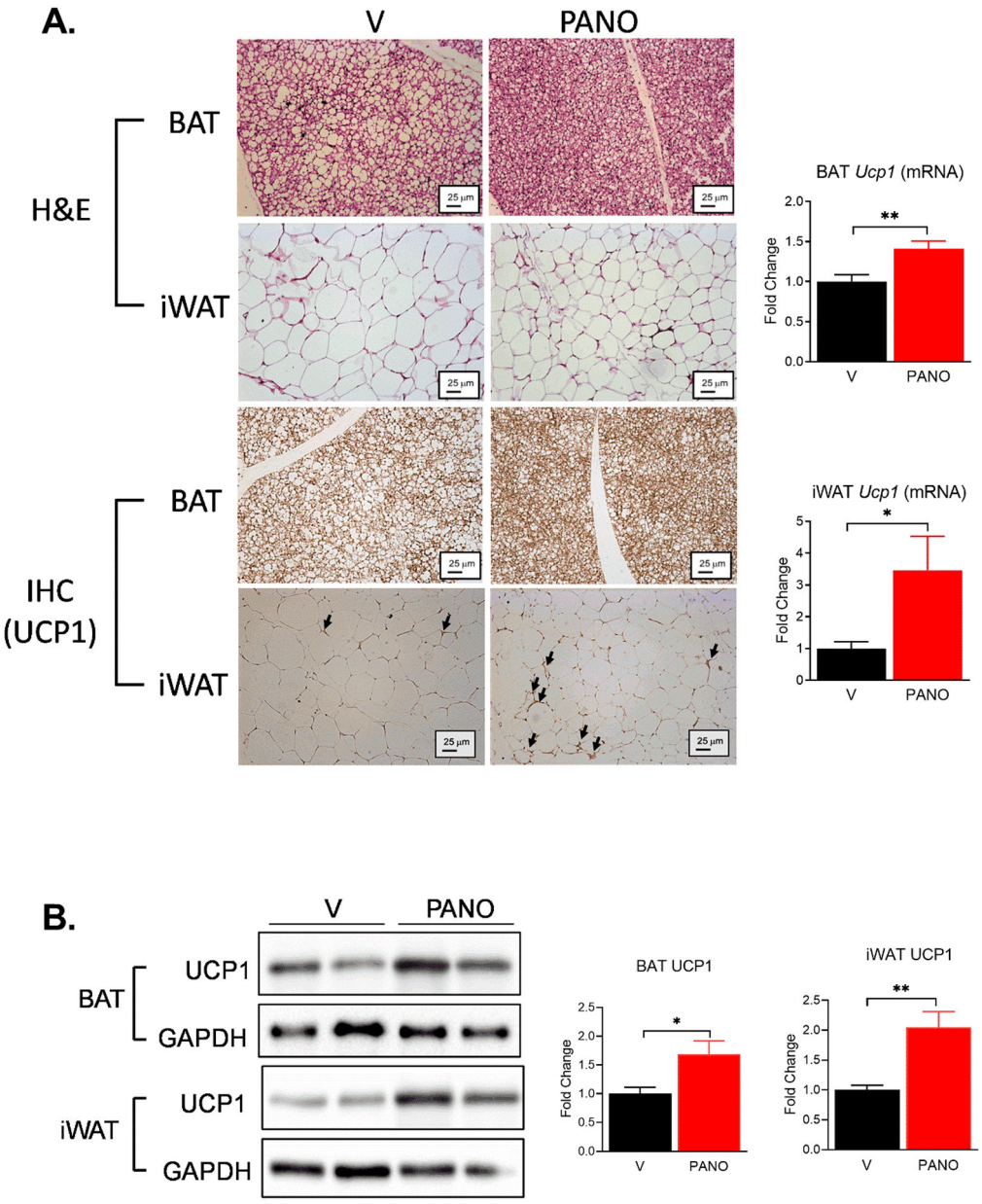

FIGURE 4. The PANO gel increased UCP1 expression in BAT and iWAT.

(A) BAT and iWAT were isolated and subjected to H& E staining (upper 4 panels). BAT and iWAT were subjected to immunohistochemistry with an anti-UCP1 antibody (lower 4 panel). The PANO gel decreased the size of the adipocytes and increased the expression of UCP1. Arrows indicate the expression of UCP1. mRNA was isolated from BAT and iWAT. The mRNA expression of *Ucp1* was evaluated. PANO increased the expression of *Ucp1*. Data are presented as mean ± SEM (n=8–10) *p<0.05, **p<0.01, and n.s. not significant. **(B)** Lysates from BAT and iWAT were extracted and subjected to Western blotting. The PANO gel increased the protein level of UCP1 in BAT and iWAT. Data are presented as mean ± SEM (n= 5 – 7). *p<0.05 and **p<0.01.

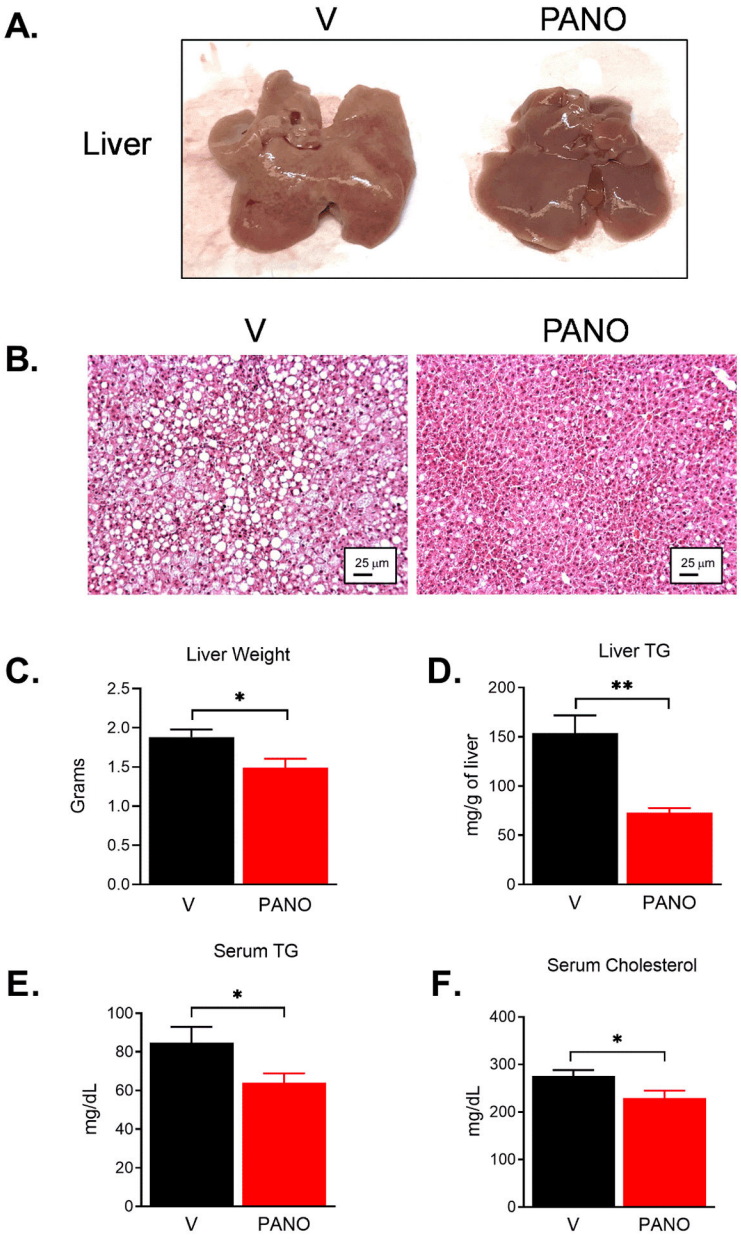

FIGURE 5. The PANO gel protects from HFD-induced non-alcoholic fatty liver.

(A) The liver isolated from HFD-fed mice showed pale color due to the accumulation of fat in the liver. **(B)** H&E staining of the liver tissue. Lipid droplets are shown as white round circles. **(C)** The isolated livers were weighed at the time of sacrifice. The PANO gel prevented the accumulation of fat and reduced liver weight. Data are presented as mean ± SEM. (n = 18 −19) **(D)** The PANO gel reduced the accumulation of triglyceride in the liver (n= 6), and **(E - F)** circulating triglyceride and cholesterol (n= 9). Data are presented as mean ± SEM. *p<0.05 and **p<0.01.

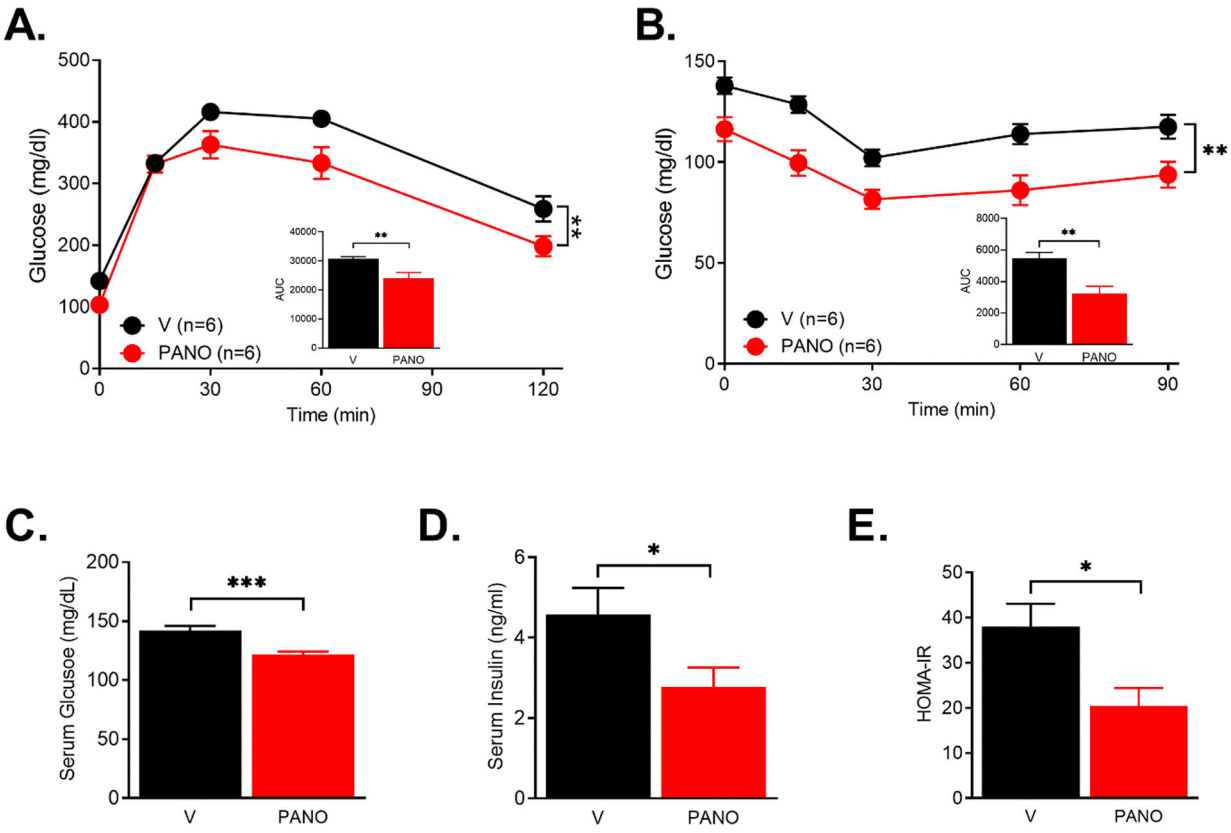

FIGURE 6. The PANO gel improved insulin sensitivity.

(A & B). V- or the PANO gel-injected HFD-fed mice were fasted for 6 hr. Glucose (2 g/kg) or insulin (0.5 U/kg) was injected and the serum glucose levels were monitored. PANO improved glucose and insulin tolerance. **p<0.01 (n=6) **(C-E)** Fasting glucose and insulin levels were measured after 6 hr of fasting. Insulin sensitivity index HOMA-IR was calculated as described in the materials and methods. Data are presented as mean ± SEM (n=11). *p<0.05, **p<0.01 and ***p<0.001.

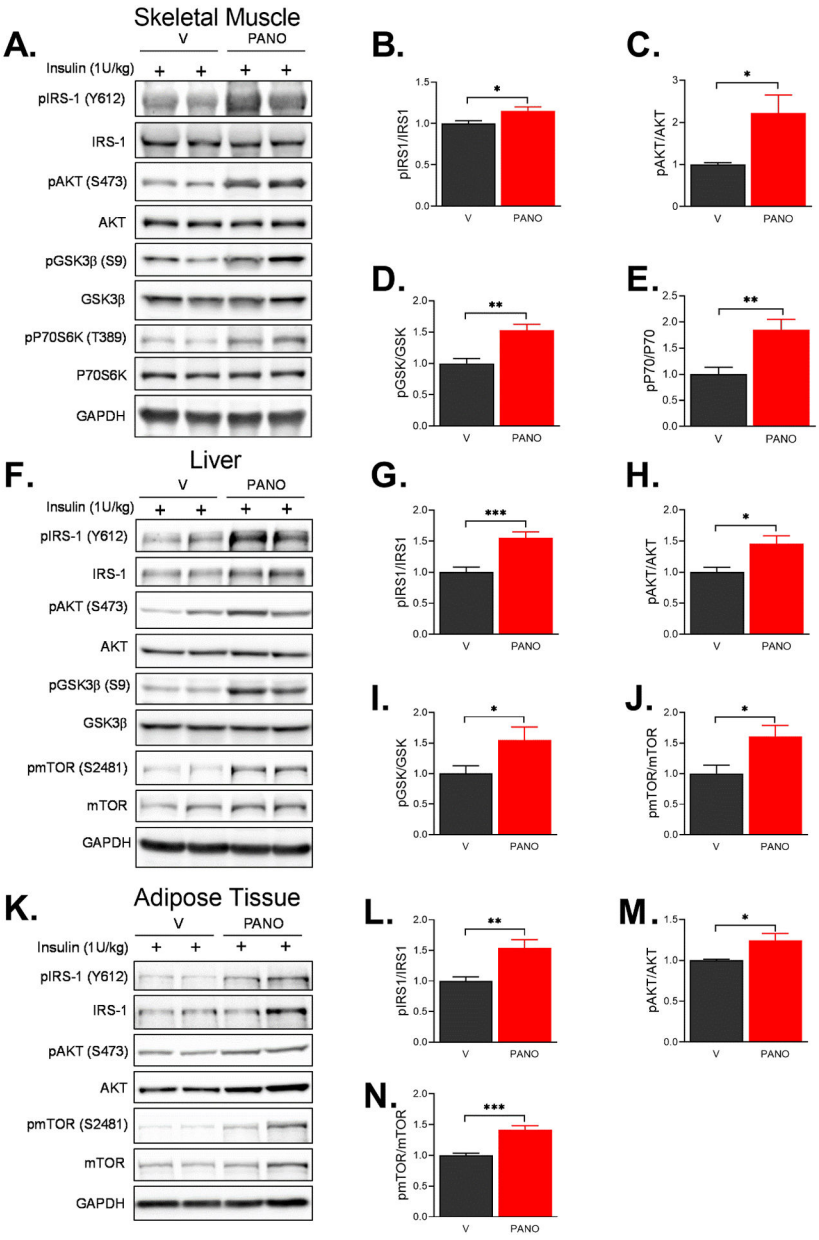

FIGURE 7. The PANO gel improved the insulin-stimulated signaling pathways.

V- or the PANO gel-injected HFD-fed mice were fasted for 6 hrs. The mice were injected with 1 U/kg insulin, and then the lysates were collected from skeletal muscle **(A-E)**, liver **(F-J)**, and eWAT **(K-N)** and subjected to immunoblottings with the indicated antibodies. The effects of the PANO gel on insulin-stimulated signaling pathways in skeletal muscle, liver, and white adipose tissue was determined. Data are presented as mean ± SEM (n=5–7). *p<0.05, **p<0.01 and ***p<0.0001.

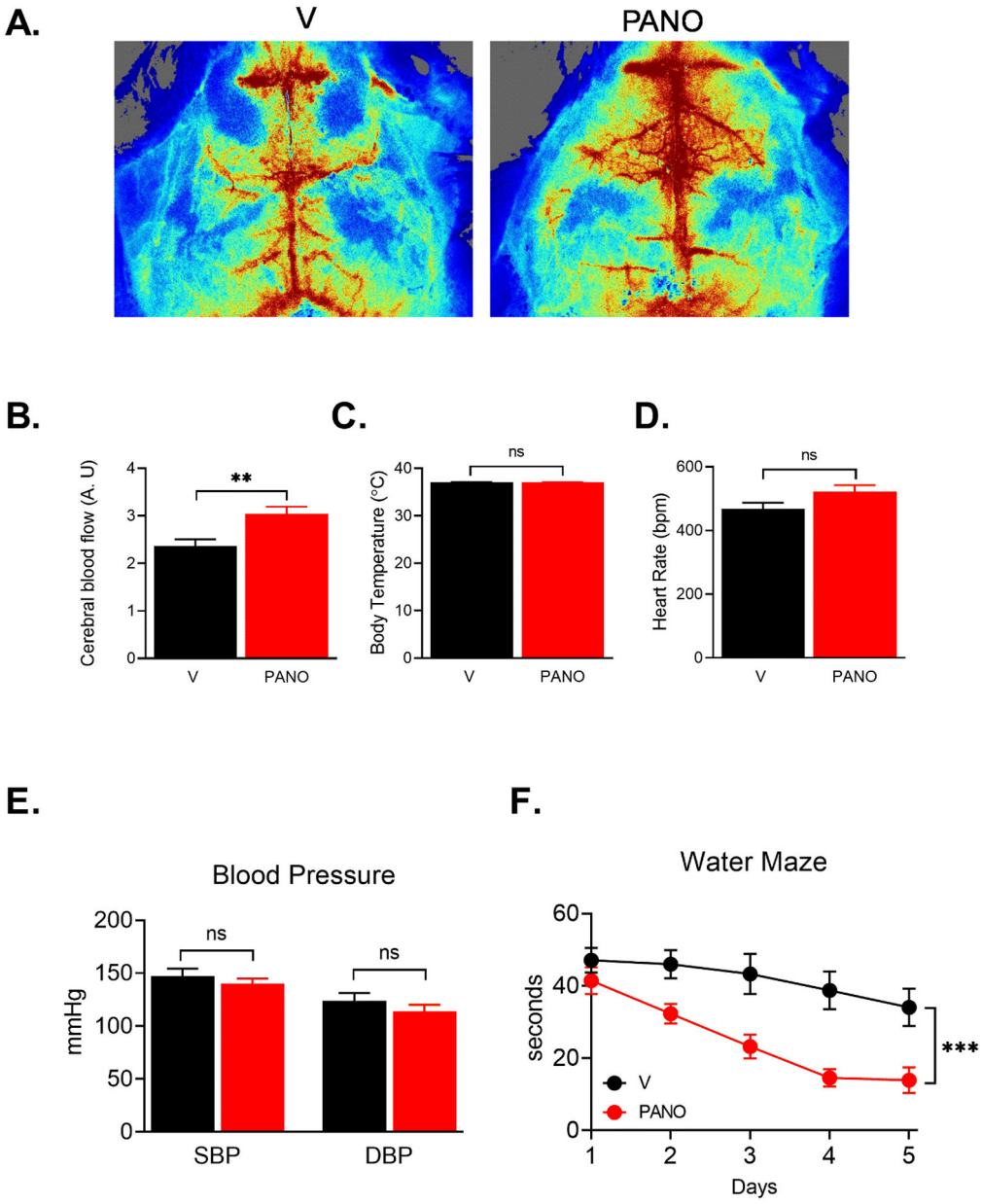

FIGURE 8. The PANO gel improved cerebral blood flow and spatial learning, and memory. **(A)** The cerebral blood flow was measured using a laser speckle contrast imager as described in the Materials and Methods. **(B-E)** Administration of the PANO gel improved cerebral blood flow while body temperature, heart rate, and blood pressure were steadily maintained. Data are presented as mean ± SEM **p<0.01 (n=7) **(F)** Morris water maze test was performed for five consecutive days. Administration of the PANO gel improved the ability of spatial learning and memory. Statistical analysis was performed with two-way repeated measurements of ANOVA combined with the Bonferroni post-doc test. Data are presented as mean ± SEM. ***p<0.001 (n=7)